ICE FORCES AGAINST ARCTIC OFFSHORE STRUCTURES

W. M. Sackinger

J. B. Johnson

Second Quarterly Report
1 June 1982
Contract No. DACA 89-82-k-0001

Submitted to

U.S. Army Cold Regions
Research and Engineering Laboratory
72 Lyme Road
Hanover, NH 03755

and to

U.S. Department of the Interior
Minerals and Management Service
MMS - Mail Stop 620
12203 Sunrise Valley Drive
Reston, VA 22091

Geophysical Institute
University of Alaska
Fairbanks, AK 99701

ICE FORCES AGAINST ARCTIC OFFSHORE STRUCTURES

W. M. Sackinger

J. B. Johnson

Second Quarterly Report
1 June 1982
Contract No. DACA 89-82-k-0001

Submitted to

U.S. Army Cold Regions
Research and Engineering Laboratory
72 Lyme Road
Hanover, NH 03755

and to

U.S. Department of the Interior
Minerals and Management Service
MMS - Mail Stop 620
12203 Sunrise Valley Drive
Reston, VA 22091

Geophysical Institute
University of Alaska
Fairbanks, AK 99701

I. BACKGROUND

This second quarterly report covers progress on the subject contract from March 1, 1982 to June 1, 1982.

As discussed in great detail in the first quarterly report, the objective of the research program is to determine the lateral forces on artificial islands and offshore structures which are subject to moving sea ice. This is the major factor governing the design of offshore facilities for petroleum production in the Beaufort, Chukchi, and Bering Seas, a frontier province which encompasses some 262 million acres with a risked mean oil equivalent of 30.8 billion barrels.

The approach taken is to measure the internal ice stress at relatively large distances from such islands, to measure the ice displacement simultaneously, and to determine the effective island width during ridgebuilding events. These events, which fracture the ice adjacent to the islands and structures, represent those time intervals when maximum total forces may be exerted on such man-made structures. They represent the extreme design condition. Although very high local forces may disturb the gravel or rock slopes of artificial islands, this can be repaired. A more significant issue is whether the lateral resistance to movement of the entire artificial island or offshore structure is sufficient to withstand the maximum total force exerted by the moving ice. Allowance must be made for the thickest ice and the highest velocity of ice movement expected during the operating life of the production facility. A thorough discussion of current practice in such designs is given in the first quarterly report.

II. EXPERIMENTAL PROGRAM

During the second quarter, calibration of the electronic data telemetry system was completed. Progress was made on the calibration of the stress sensors within ice blocks, as well. A loading press capable of handling cubic ice samples nineteen inches on each side was made available to us at no charge by the Research Division of the Alaska Department of Transportation and Public Facilities. An aluminum fixture was designed to produce ice blocks which would fit within this uniaxial loading press. This ice block mold was constructed, and successfully tested. Special waterproofing coatings for the ice gauges were tested and successfully withstood brine immersion for several weeks with no deterioration. The uniaxial gauges were coated, and fixtured to be frozen into the ice blocks.

Additional theoretical developments were completed during the second quarter which pointed to the need for calibration of the uniaxial sensors at several angles other than 0°, 45°, and 90°. As is described in the next chapter, to properly ascertain the direction of the principal stresses from uniaxial stress gauge data, the calibration of the stress concentration factor $\alpha(\theta)$ must be obtained experimentally. Angles of 30° and 60° are also planned for the calibration sequence. Such tests are proceeding during the next quarter.

A closer examination of the system alternatives for ice positioning revealed that two competing systems, the Motorola Mini-Ranger and the Racol-Decca, should be evaluated. A comparison of the two systems, detail-by-detail, is being done and will be completed soon.

It appears that the installation of either system will be for a field season of several months duration, implying that it will be more

economical to purchase the positioning system rather than obtaining it on a lease arrangement.

Discussions with Shell Oil Company personnel about the possibilities of 1982-83 deployment near their SEAL artificial island location in 39 feet of water resulted in a favorable response, and formal Shell management approval has been requested.

An initial theoretical analysis was completed for both types of gauges, and it is presented in the following section.

III. DETERMINING STRESSES AND STRAINS IN AN ICE SHEET USING A UNIAXIAL STRESS SENSOR AND A TRI-AXIAL STRAIN SENSOR

Two different methods will be used in this study to measure stresses and strains in an ice sheet. Stresses in a biaxial field will be measured using a rosette of three stress transducers oriented at 45° from one another. This configuration can be used to resolve the direction and magnitudes of an acting two-dimensional stress field. The basic assumption for using a rosette of sensors is that stresses act in the plane of an ice sheet and that out-of-plane stresses are negligible. This assumption has not been proven by past measurements. An effort also will be made during this study to measure the three-dimensional strain field for an ice sheet and infer the corresponding stress field for short-term loading. The in-plane and out-of-plane strains/stresses can be determined from the three-dimensional measurements.

A brief description of the two sensors used in this study and the methods used to interpret their output is presented in the following. The calibration requirements and interpretation methods for the uniaxial stress sensor are presented first. The equations needed to interpret the tri-axial strain transducer are described in Section 2.

Uniaxial Stress Sensor

The uniaxial stress sensor is a stiff transducer designed to measure stresses in ice. The operation and design characteristics of the sensor have been described previously (Nelson and others, 1977). Nelson showed that the sensor exhibits strong stress concentration and transverse sensitivity characteristics. He assumed that the stress concentration factor for the sensor was constant with respect to the orientation of the sensor to the principal stress direction. Savin (1961), however, has shown that an inclusion with the general shape of such a gauge has a stress concentration factor that is dependent on the orientation of the sensor with respect to the principal stresses. This section presents the basic equations needed to interpret the results of the uniaxial gauge and discusses the required calibrations for the sensor.

Calibration tests for the uniaxial sensor have demonstrated that it has a large stress concentration factor and transverse sensitivity (Nelson and others, 1977). This can be described (for a uniaxial stress field, $\sigma_2 = 0$) by

(1) $\sigma_{om} = \alpha \sigma_1 \cos^2\theta + \beta \sigma_1 \sin^2 \theta$ where

σ_{om} is the stress determined from sensor measurements, α is the stress concentration factor σ_{om}/σ_1, σ_1 is the applied stress, β is the transverse sensitivity coefficient σ_{om}/σ_1 at $\Theta = 90°$ and Θ is the orientation of the sensor with respect to the applied stress field (Figure 1).

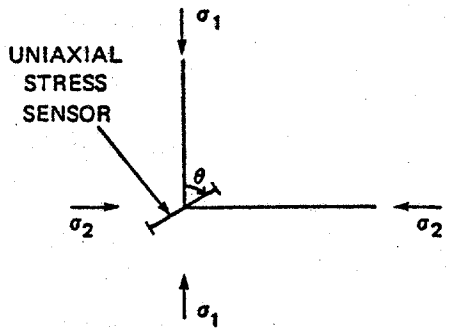

Figure 1

The transverse sensitivity coefficient is primarily the result of a Poisson's ratio effect in the ice and can be assumed to be a constant value. The stress concentration factor, α, does, however, depend on Θ and this dependence can influence the interpretation of results. Both β and $\alpha(\Theta)$ must be determined during the calibration of the sensor if meaningful results are to be obtained. The transverse sensitivity can be determined by orienting the sensor at 90° to the applied load and calculating β from

(2) $\beta = \sigma_{0m}/\sigma_1$ at $\theta = 90°$.

The stress concentration coefficient, $\alpha(\theta)$, must be determined over the range $0 \leq \Theta < \pi/2$ so that the measured stress can be used to calculate the applied stress. Once β has been determined equation 1 can be used to calculate $\alpha(\Theta)$ at various orientations to the applied field

(3) $\alpha(\theta) = (\sigma_{0m} - \beta\ \sigma_1 \sin^2 \theta)/(\sigma_1 \cos^2 \theta)$ @ $0 \leq \theta < \pi/2$

(4) $\alpha(\pi/2) = 0$ @ $\theta = \pi/2$

The coefficients $\alpha(\Theta)$ and β can now be determined from a set of calibration tests and equations 2 and 3.

An additional set of equations is needed to interpret the readings from sensors imbedded in ice that are subjected to biaxial loading.

Equation 1 can be expanded to include the effects of a biaxial stress field

(5) $\sigma_{om} = \alpha(\theta)\ \sigma_1 \cos^2\theta + \alpha((\pi/2)-\theta)\ \sigma_2 \sin^2\theta + \beta(\sigma_1 \sin^2\theta + \sigma_2 \cos^2\theta).$

This can be rewritten as .

(6) $\sigma_{om} = [(\alpha(\theta)+\beta)\sigma_1+(\alpha((\pi/2)-\theta)+\beta)\sigma_2]/2 + [(\alpha(\theta)-\beta)\sigma_1-(\alpha((\pi/2)-\theta)-\beta)\sigma_2]\ (\cos\theta)/2$

An array of three sensors is needed to resolve a biaxial stress field in ice. Typically the sensors are oriented at 45° angles from each other (Figure 2).

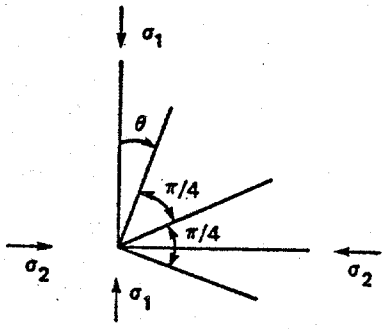

Figure 2

The stresses acting on each sensor can be determined using equation 6.

(7) $\sigma_{om1} = [(\alpha(\theta)+\beta)\sigma_1+(\alpha_2((\pi/2)-\theta)+\beta)\sigma_2]/2 + [(\alpha(\theta)-\beta)\sigma_1-(\alpha((\pi/2)-\theta)-\beta)\sigma_2]\ (\cos 2\theta)/2$

(8) $\sigma_{om2} = [(\alpha(\theta + (\pi/4)) + \beta)\sigma_1 + (\alpha((\pi/4)-\theta)+\beta)\sigma_2]/2 + [(\alpha(\theta+\pi/4)-\beta)\sigma_1-(\alpha(\pi/4-\theta)-\beta)\sigma_2]\ (\cos 2\ (\theta + (\pi/4)))/2$

(9) $\sigma_{om3} = [(\alpha(\theta+(\pi/2))+\beta)\sigma_1+(\alpha(\theta)+\beta)\sigma_2]/2 + [(\alpha(\theta+(\pi/2))-\beta)\sigma_1-(\alpha(\theta)-\beta)\sigma_2]\ (\cos 2\ (\theta+(\pi/2)))/2$

It is apparent from equations 7-9 that the system of equations for a three sensor array can be complex. There is no straightforward way to eliminate the different α values from the equation to solve for Θ and then for σ_1 and σ_2. At this point one should refer to the calibration curve for α to determine how significantly $\alpha(\Theta)$ varies with Θ. If the variation is slight then it may be worthwhile to assume that $\alpha(\Theta)$ is constant and solve for Θ, σ_1 and σ_2 in the usual fashion. In such a case equations 7-9 can be rewritten as

$$(10)\quad \sigma_{om1} = (\alpha+\beta)\,(\sigma_1+\sigma_2)/2 + (\alpha-\beta)\,(\sigma_1-\sigma_2)\cos 2\theta/2$$

$$(11)\quad \sigma_{om2} = (\alpha+\beta)(\sigma_1+\sigma_2)/2 - (\alpha-\beta)\,(\sigma_1-\sigma_2)\sin 2\theta/2$$

$$(12)\quad \sigma_{om3} = (\alpha+\beta)\,(\sigma_1+\sigma_2)/2 - (\alpha-\beta)\,(\sigma_1-\sigma_2)\cos 2\theta/2$$

Equations 10-12 can now be solved giving

$$(13)\quad \text{Tan } 2\theta = (\sigma_{om1} - 2\,\sigma_{om2} + \sigma_{om3})/(\sigma_{om1} - \sigma_{om3})$$

$$(14)\quad \sigma_1 + \sigma_2 = (\sigma_{om} + \sigma_{om3})/(\alpha+\beta)$$

$$(15)\quad \sigma_1 - \sigma_2 = [(\sigma_{om1}-\sigma_{om3})^2 + (\sigma_{om1} + \sigma_{om3} - 2\sigma_{om2})^2]^{1/2}/(\alpha-\beta)$$

However, if $\alpha(\Theta)$ does vary strongly with orientation then Θ may be determined by some other means (for example separate surface strain measurements). Once Θ is known, then σ_1 and σ_2 can be determined from two sensor readings and any two of equations 7-9. For two sensors oriented at 90 degrees from each other a solution of

$$\begin{bmatrix} [(\alpha(\theta)+\beta) + (\alpha(\theta)-\beta)\cos 2\theta]/2 & [(\alpha((\pi/2)-\theta)+\beta)-(\alpha((\pi/2)-\theta)-\beta)\cos 2\theta]/2 \\ [\alpha(\theta+(\pi/2))+\beta)+(\alpha(\theta+(\pi/2))-\beta)\cos 2(\theta+(\pi/2))]/2 & [(\alpha(\theta)+\beta)-(\alpha(\theta)-\beta)\cos 2(\theta+(\pi/2))]/2 \end{bmatrix} \begin{bmatrix} \sigma_1 \\ \sigma_2 \end{bmatrix} = \begin{bmatrix} \sigma_{om1} \\ \sigma_{om2} \end{bmatrix}$$

will give α_1 and α_2.

Circular Ribbon and Triaxial Strain/Stress Sensor

The triaxial strain/stress sensor consists of three circular ribbons of metal to which strain sensors have been attached at 120° spacings. By monitoring the tangential strain in a hoop, the principal strains/stresses in the plane of the hoop can be determined. The complete strain/stress field in a three-dimensional body can be determined when three hoops oriented in different directions are imbedded in the object.

Two separate solution sets are needed to determine the three-dimensional strain/stress field from the ribbon hoops. The first set of equations is used to determine the principal strains and their orientations in the plane of the hoop for each sensor. These measurements are then used to develop a system of four equations with three unknowns. The three unknowns and estimates of their accuracy are determined using standard matrix inversion techniques.

The solutions for resolving the strain/stress field from tangential strain measurements using the ribbon sensors are presented below. The formulas needed to resolve the two-dimensional principal strains are treated first. Next the equations for resolving the three-dimensional strain field are presented and used to calculate stresses assuming an elastic response for ice.

Determining Principal Strains in the Plane of a Ribbon Sensor in Ice

The thin flexible nature of the ribbon sensor means that one can assume that the sensor deforms with the ice (that is the sensor responds to strain). The deformation of the sensor can then be related to the principal strains in the ice by

$$(16) \quad \varepsilon_r = (\varepsilon_p+\varepsilon_q)/2 + (\varepsilon_p-\varepsilon_q)\ (\cos 2\theta)/2,$$

$$(17) \quad \varepsilon_\theta = (\varepsilon_p+\varepsilon_q)/2 - (\varepsilon_p-\varepsilon_q)\ (\cos 2\theta)/2$$

$$(18) \quad \varepsilon_{r\theta} = -(\varepsilon_p-\varepsilon_q)\ (\sin 2\theta)/2,$$

where ε_r, ε_θ, $\varepsilon_{r\theta}$ are the radial, tangential and shear strains in the ribbon sensor. The principal strains in the ice are ε_p and ε_q where $\varepsilon_p > \varepsilon_q$ and Θ is the angle between the p axis and the r axis (Figure 3).

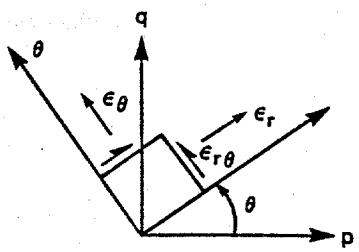

Figure 3

Equation 17 can be used to resolve the principal strains using tangential strain sensors on a hoop. For three strain sensors spaced 120° apart equation 17 provides three equations

$$(19) \quad \varepsilon_{\theta 1} = (\varepsilon_p+\varepsilon_q)/2 - (\varepsilon_p-\varepsilon_q)\ (\cos 2\theta)/2$$

$$(20) \quad \varepsilon_{\theta 2} = (\varepsilon_p+\varepsilon_q)/2 + (\varepsilon_p-\varepsilon_q)\ ((\cos 2\theta)/2-\sqrt{3}/2\ \sin 2\theta)/2$$

$$(21) \quad \varepsilon_{\theta 3} = (\varepsilon_p+\varepsilon_q)/2 + (\varepsilon_p-\varepsilon_q)\ ((\cos 2\theta)/2 + \sqrt{3}/2\ \sin 2\theta)/2$$

where $\varepsilon_{\theta 1}$, $\varepsilon_{\theta 2}$, $\varepsilon_{\theta 3}$ refer to the strains at locations 1, 2 and 3 in Figure 4

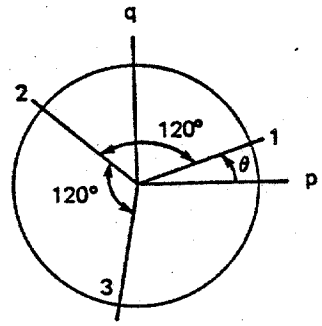

Figure 4

The above three equations can be solved for the principal strains ε_p and ε_q and the orientation θ from an arbitrary set of axes.

(22) $\Theta = 1/2 \ \mathrm{Tan}^{-1} \left[\sqrt{3} \ (\varepsilon_{\theta 2}-\varepsilon_{\theta 3})/(2\varepsilon_{\theta 1}-\varepsilon_{\theta 2}-\varepsilon_{\theta 3})\right]$

(23) $\varepsilon_p+\varepsilon_q = 2/3 \ (\varepsilon_{\theta 1} + \varepsilon_{\theta 2} + \varepsilon_{\theta 3})$

(24) $(\varepsilon_p-\varepsilon_q) = [4/3 \ (\varepsilon_{\theta 2}-\varepsilon_{\theta 3})^2 + 4/9 \ (2\varepsilon_{\theta 1}-\varepsilon_{\theta 2}-\varepsilon_{\theta 3})^2]^{1/2}.$

Equations 22-24 are used to solve for the principal strains in the plane of each sensor. These can then be used to determine the three-dimensional strain field by using the relations

(25) $\varepsilon_{y'} = \ell_2^2\varepsilon_x+m_2^2 \ \varepsilon_y+n_2^2 \ \varepsilon_z+2m_2n_2 \ \varepsilon_{xy} + 2n_2\ell_2 \ \varepsilon_{zx}+ 2\ell_2m_2 \ \varepsilon_{xy}$

(26) $\varepsilon_{z'} = \ell_3^2 \ \varepsilon_x+ m_3^2 \ \varepsilon_y+n_3^2 \ \varepsilon_z+2m_3n_3 \ \varepsilon_{xy}+2n_3\ell_3 \ \varepsilon_{zx} + 2\ell_3m_3 \ \varepsilon_{xy}$

(27) $\varepsilon_{y'z'} = \ell_2\ell_3 \ \varepsilon_x+m_2m_3 \ \varepsilon_y+n_2n_3 \ \varepsilon_z+(m_2n_3+m_3n_2) \ \varepsilon_{yz}+ (n_2\ell_3+n_3\ell_2) \ \varepsilon_{zx}+(\ell_2m_3+\ell_3m_2) \ \varepsilon_{xy}$

where $\varepsilon_{y'}$, $\varepsilon_{z'}$ and $\varepsilon_{y'z'}$ are the normal and shear strains to a plane whose direction cosines from the reference coordinate system Oxyz are given by (ℓ_1, m_1, n_1), $(\ell_2, m_2 \ n_2)$, (ℓ_3, m_3, n_3) (Figure 5) (Jaeger and Cook, 1979).

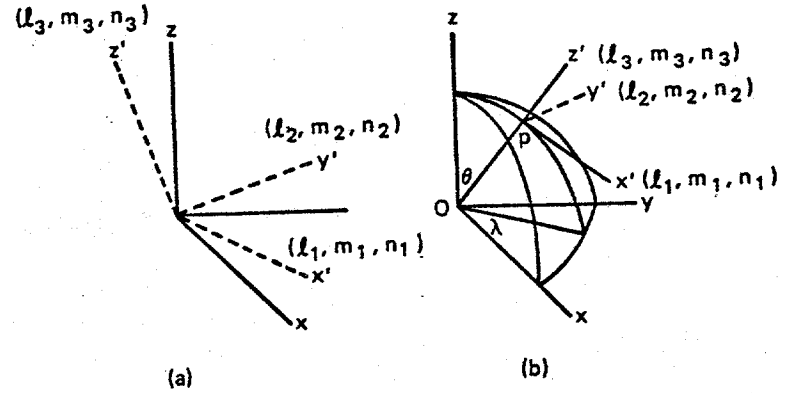

Figure 5
(From Jaeger and Cook, 1979)

Equations 25-27 are used by arbitrarily setting a reference coordinate system Oxyz to correspond to one of the principal axes determined from ribbon sensor measurements and equations 22-24. The strains ε_y, ε_z are known and $\varepsilon_{yz} = 0$ for the principal strain axis system. In the following presentation ε_{y1}, ε_{z1}, $\varepsilon_{zy1} = 0$ refer to the strains in the principal strain system determined from measurements of ribbon sensor 1. The principal strains from the remaining sensors are ε_{y2}, ε_{z2}, $\varepsilon_{yz2} = 0$; ε_{y3}, ε_{z3}, $\varepsilon_{zy3} = 0$ for ribbon sensors 2 and 3 respectively. Using Equations 25-27 gives

$$(28) \quad \varepsilon_{y2} = \ell_1^2\varepsilon_x + m_1^2\varepsilon_{y1} + n_1^2\varepsilon_{z1} + 2n_1\ell_1\varepsilon_{zx} + 2\ell_1 m_1\varepsilon_{xy}$$

$$(29) \quad \varepsilon_{z2} = \ell_2^2\varepsilon_x + m_2^2\varepsilon_{y1} + n_2^2\varepsilon_{z1} + 2n_2\ell_2\varepsilon_{zx} + 2\ell_2 m_2\varepsilon_{xy}$$

$$(30) \quad 0 = \ell_1\ell_2\varepsilon_x + m_1 m_2\varepsilon_{y1} + n_1 n_2\varepsilon_{z1} + (n_1\ell_2 + n_2\ell_1)\varepsilon_{zx} + (\ell_1 m_2 + \ell_2 m_1)\varepsilon_{xy}$$

which are three equations for unknowns ε_x, ε_{xy}, ε_{zx}. However, the determinant for these equations vanishes, so that they are not independent. The measurements from the third ribbon sensor can be used to provide the additional equations

$$(31) \quad \varepsilon_{y3} = \ell_3^2\varepsilon_x + m_3^2\varepsilon_{y1} + n_3^2\varepsilon_{z1} + 2n_3\ell_3\varepsilon_{zx} + 2\ell_3 m_3\varepsilon_{xy}$$

$$(32) \quad \varepsilon_{z3} = \ell_4^2\varepsilon_x + m_4^2\varepsilon_{y1} + n_4^2\varepsilon_{z1} + 2n_4\ell_4\varepsilon_{zx} + 2\ell_4 m_4\varepsilon_{xy}$$

(33) $0 = \ell_3 \ell_4 \varepsilon_x + m_3 m_4 \varepsilon_y + n_3 n_4 \varepsilon_{z1} + (n_3 \ell_4 + n_4 \ell_3) \varepsilon_{zx} +$

$(\ell_3 m_4 + \ell_4 m_3) \varepsilon_{xy}$

Equations 28, 29, 31 and 32 can now be used to solve for the three unknowns and also give an estimate to the accuracy of the measurement as described in Fung, 1977). The strain field for the body is given by

$$\varepsilon_{ij} = \begin{bmatrix} \varepsilon_x & \varepsilon_{xy} & \varepsilon_{xz} \\ \varepsilon_{yx} & \varepsilon_{y1} & 0 \\ \varepsilon_{xz} & 0 & \varepsilon_{z1} \end{bmatrix} \qquad i,j = 1,2,3$$

The principal strains in three dimensions are now determined in the standard fashion as follows. First solve

$$|\varepsilon_{ij} - E_k \delta_{ij}| = \begin{bmatrix} (\varepsilon_x - E) & \varepsilon_{xy} & \varepsilon_{xz} \\ \varepsilon_{yx} & (\varepsilon_{y1} - E) & 0 \\ \varepsilon_{xz} & 0 & (\varepsilon_{z1} - E) \end{bmatrix} = 0$$

which is a cubic equation in E. E has three real roots, which are the principal strain magnitudes, such that $\varepsilon_1 > \varepsilon_2 > \varepsilon_3$. The orientation of the principal strain axis system from the Oxyz system is determined by the direction cosines ℓ_{pK}, m_{pK}, n_{pK}. These are determined by solving

$$(\varepsilon_{ij} - \varepsilon(K)\, \delta_{ij}) n_j(K) = \begin{bmatrix} (\varepsilon_x - \varepsilon_K) & \varepsilon_{xy} & \varepsilon_{xz} \\ \varepsilon_{yx} & (\varepsilon_{y1} - \varepsilon_K) & 0 \\ \varepsilon_{zx} & 0 & (\varepsilon_{z1} - \varepsilon_K) \end{bmatrix} \begin{bmatrix} \ell_{pK} \\ m_{pK} \\ n_{pK} \end{bmatrix} = 0$$

where K = 1, 2, 3

which gives three sets of direction cosines ℓ_{p1}, m_{p1}, n_p, ℓ_{p2}, m_{p2}, n_{p2}, ℓ_{p3}, m_{p3}, n_{p3}, describing the orientation of the principal stress axis from the Oxyz axis.

The principal strains and direction cosines completely describe the three-dimensional strain field of the ice. If a further assumption is made that the deformation in the ice is of short duration and not permanent then

the ice can be treated as an elastic material. The three-dimensional principal stress field can be calculated from

$$\sigma_1 = \lambda\ (\varepsilon_1+\varepsilon_2+\varepsilon_3)+2\mu\ \varepsilon_1$$

$$\sigma_2 = \lambda\ (\varepsilon_1+\varepsilon_2+\varepsilon_3)+2\mu\ \varepsilon_2$$

$$\sigma_3 = \lambda\ (\varepsilon_1+\varepsilon_2+\varepsilon_3)+2\mu\ \varepsilon_3$$

where λ and μ are material properties of the ice which is assumed to be isotropic, homogeneous and behave in a linear elastic fashion. The direction cosines for the stress system are colinear to those of the principal strain system.

The results of this development assume that infinitesimal strain theory is valid. If the ice experiences significant plastic deformation then the result of this section cannot be used to determine the stress from the output of the ribbon strain sensors, and further analysis is needed. The anisotropy of sea ice should also be taken into account in a more detailed analysis.

IV. PLANS FOR THIRD QUARTER

The sequence of calibrations of the uniaxial and the ring gauges will continue in ice blocks. An evaluation of the positioning system alternatives will be completed.

Theoretical analysis of the uniaxial gauge behavior will concentrate upon a computer method of solving for direction and magnitude of principal stresses once the data from the gauges is provided. Some additional attention will be given to specific solutions for the stresses as derived from data taken with the array of three ring gauges. The questions of plastic flow in ice, and also the known anisotropy of sea ice, will be considered insofar as they would affect the output of the gauges and its proper interpretation.

IV. REFERENCES

Fung, Y.C., 1969. A first course in continuum mechanics, Prentice-Hall Inc., 2nd Ed., 1979, pp. 340.

Jaeger, J.C. and N.G.W. Cook, 1969. Fundamentals of rock mechanics, Chapman and Hall, London, 3rd Ed., 1979, pp. 593.

Savin, G.N., 1961. Stress concentrations around holes, Pergamon Press, New York, 430 pp. Translated from the Russian "Kontsentratsiya Napryazhenii Okolo Otverstii" (Moscow/Leningrad, Gostekhteoretizdat, 1951.)

Nelson, R.D., Tauriainen, M. and Borghorst, J. 1977. Techniques for measuring stress in sea ice, Alaska Sea Grant Report No. 77-1, 65 pp.